

First Simultaneous Acquisition of a Clinical SPECT-MRI Brain INSERT

Ashley J. Morahan, Ilenia D’Adda, *Member, IEEE*, Kjell Erlandsson, Marco Carminati, *Senior Member, IEEE*, Marilena Rega, Darren Walls, Carlo Fiorini, *Senior Member, IEEE*, Brian F. Hutton, *Senior Member, IEEE*

Abstract— The INSERT (INtegrated SPECT/MRI for Enhanced stratification of brain tumours in Radio-chemoTherapy) is currently the only MRI-compatible SPECT stationary system for clinical application, in particular for brain multimodal imaging with an inner bore of 28 cm and a field of view of 20 cm (transaxial) \times 10 cm (axial). The intrinsic spatial resolution is 1 mm and the extrinsic one is 10 mm. This modular scanner fits in an unmodified MRI scanner and is a scale-up of a smaller preclinical version, whose mutual compatibility with MRI was extensively characterized. It is composed of 20 detection modules (with 8-mm thick CsI:Tl scintillators of 5 cm \times 10 cm area read by an array of SiPM) and a massive multi-mini slit-slat collimator, realized in tungsten. Here we report the first demonstration of successful simultaneous SPECT/MRI acquisition of phantoms (hot rods) using a commercial transceiver coil in a Siemens Biograph mMR scanner.

I. INTRODUCTION

THE INSERT is a clinical single photon emission computed tomography (SPECT) system, designed for integration with clinical Magnetic Resonance Imaging (MRI) [1]. It addresses in particular multi-modal imaging for brain oncology with sub-cm extrinsic spatial resolution. The scanner is comprised of a stationary partial ring of 20 compact detectors made of Cesium Iodide (CsI:Tl) scintillators (50 mm \times 100 mm, and thickness of 8 mm) readout by a total of 1440 Silicon Photomultiplier (SiPM RGB-HD by Fondazione Bruno Kessler) [2]. The INSERT scanner makes use of a novel multi-slit-slat (MSS) collimator, specifically designed for this application, in order to minimize its thickness and tackle the sensitivity/spatial resolution trade-off [3]. It was fabricated aligning 6’000 pieces of tungsten (to reduce eddy currents) by Nuclear Fields [4] for a total weight of about 50 kg. The SPECT axial field of view (FoV) is 10 cm and the transaxial FoV is about 20 cm. The MRI-compatibility of electronics was successfully verified on a pre-clinical system [5]. The complete system has undergone initial testing as a stand-alone SPECT scanner [4] showing a 1 mm intrinsic

resolution (with a maximum likelihood reconstruction) and 15% energy resolution at 140 keV. The capability of Depth-of-Interaction (DOI) estimation (classification into four DOI depths in the crystal) by means of a statistical method was also demonstrated [6]. Furthermore, potential for data reduction and 2D position estimation by means of fast machine learning classifiers, embeddable in the FPGAs acquiring data from each individual module and transmitting then in the optical bus, has been recently achieved [7], paving the way to further increases of the FoV with reduced hardware overhead.

Here we report the first simultaneous SPECT-MRI acquisition (Fig. 1) in a clinical MRI at the University Hospital of the University College London (UK).

II. MRI ACQUISITION

The INSERT was installed in a Siemens Biograph mMR [8], with 3-T field, using a Dual Tuned Quadrature Head Coil (by Rapid Biomedical). The MRI quality was tested with a T2 weighted Gradient Echo (GRE) sequence. This sequence was chosen for its compatibility with the clinical INSERT system. The INSERT scanner is based on its preclinical predecessor, which components were validated for use of simultaneous SPECT-MRI [5]. The preclinical INSERT was developed with a customised MRI coil (a transceiver bird cage), which was shielded and tuned for simultaneous imaging. The clinical system does not have a customised coil available, resulting in

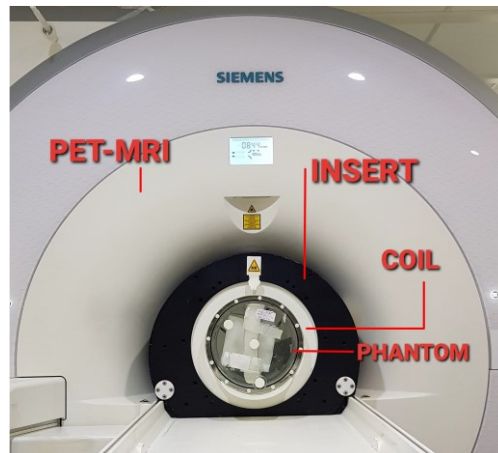


Fig. 1. The INSERT clinical prototype (42 cm height, 65 cm diameter, and 28 cm of internal bore) placed in the bore of the Siemens Biograph mMR PET-MR system for simultaneous SPECT/MRI scanning.

Manuscript received December 9, 2022.

A.J. Morahan, K. Erlandsson, M. Rega, D. Walls, and B.F. Hutton are with the Institute of Nuclear Medicine, University College London and University College Hospital, London NW1 2BU, UK (email: ashley.morahan.17@ucl.ac.uk).

I. D’Adda, M. Carminati and C. Fiorini are with Dipartimento di Elettronica, Informazione e Bioingegneria, Politecnico di Milano and INFN Sez. Milano, Milano 20133 Italy (email: marco1.carminati@polimi.it).

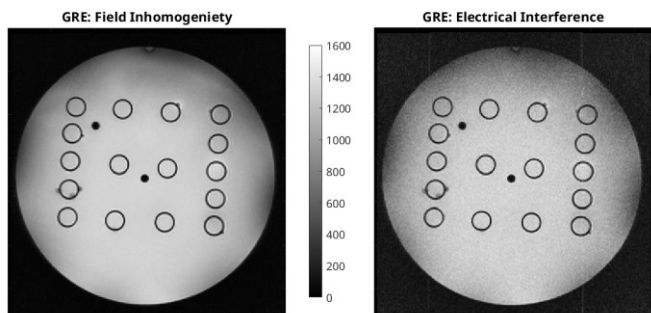


Fig. 2. The MSS collimator reduces field homogeneity on the top and sides of the FoV due to its partial ring design (left). External frequencies induce a line artefact in the MRI reconstruction (right). The GRE sequence is set to overcome interference from the SPECT electronics and collimator through shimming and averaging the signal.

the use of an off the shelf MRI coil with no copper shielding. As expected, without the correct shielding, the INSERT is unable to operate in the presence of certain levels of radio frequency (RF) energy and waveforms, thus limiting the choice of MRI sequences which can be used for simultaneous scanning.

There are two main compatibility issues that arise in the MRI, due to the SPECT system. The bulk of the INSERT metal collimator, can affect magnetic field homogeneity, and the presence of electrical signals can interfere with normal MRI operation. Figure 2 demonstrates the GRE sequences when acquiring data along side the INSERT system. The field inhomogeneity results in a loss of signal at the edges of the FoV, this is seen in the shadow artefact close to the collimator position. Field shimming is used to counter the effect and improve homogeneity. When the INSERT is powered, the electrical signal can induce interfering frequencies which result in noise and a line artefact in the GRE images. MRI sequences with higher signal than the GRE may be more robust to these artefacts. However, as stated, the RF in these sequences cannot be operated alongside the INSERT system for simultaneous acquisition. Taking more signal averages can reduce the noise at the cost of acquisition time.

III. SPECT PERFORMANCE

Although the INSERT is designed for use in a clinical MRI system, the Biograph mMR is a PET-MRI system. The presence of Lutetium-176 in the PET $Lu_2SiO_5:Ce$ (LSO) detectors poses an additional problem for the SPECT system which is designed for lower energy emission. We assess the impact of ^{176}Lu emission during data acquisition. The ^{176}Lu had a low count-rate within the 140 keV photopeak energy window. An additional energy window can be used to estimate the ^{176}Lu background for subtraction. The result of background subtraction removes an average of 5% of the total counts in a given acquisition.

The INSERT partial ring design has been reported on [9]; here phantom rotation is used to improve tomographic reconstruction and produce a full ring reconstruction. The rotated acquisition requires two phantom positions to be registered into a common space. Each SPECT acquisition is

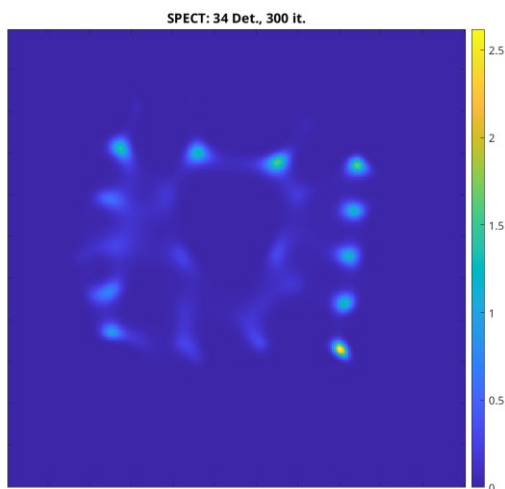


Fig. 3. The left and right columns of test tubes contain similar activity concentrations. The centre test tubes have 1, 2 and 3 part concentrations. The tubes are placed in a 20 cm cylindrical phantom to fill the SPECT FoV. Image reconstructed with ^{176}Lu subtraction.

reconstructed and a transformation is calculated to register the images. The transformation is applied to a final tomographic reconstruction, which registers all acquired data in to a common space. With the acquisition of simultaneous SPECT-MRI data, the MRI images can be used to aid the reconstruction process. An MRI to MRI registration provides a transformation between the two acquisitions which is used to translate the SPECT data from each rotation angle. Fig. 4 exhibits the reconstruction pipeline which produces the full ring reconstruction. A phantom with 16 test tubes (of 1 cm diameter) was imaged on the dual system. The test tubes were filled with either 1, 2, or 3 parts concentration of 4 MBq doses, totalling 64 MBq. The rotated positions were transformed, and tomographic image reconstruction was carried out with 300 iterations of an MLEM algorithm, the image FoV is $20\text{ cm} \times 20\text{ cm}$ (Fig. 3).

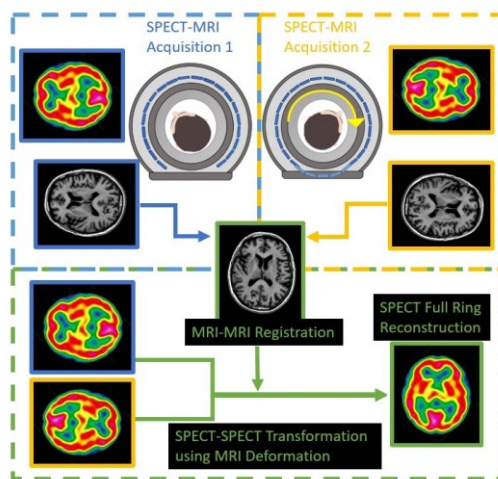


Fig. 4. The reconstruction pipeline demonstrates the use of MRI to MRI registration to aid in the SPECT reconstruction. A single acquisition can collect data from 20 detector positions, the "Full Ring Reconstruction" is able to use data from 40 positions.

IV. SIMULTANEOUS SPECT-MRI

The MRI and SPECT images were aligned using the positions of the test tubes, and combined. The fused SPECT and MRI images are displayed in Fig. 5. The SPECT image was reconstructed with 34 angles with the rotated acquisition, due to detector faults, 3 angles from each acquisition are omitted from the reconstruction. These results are preliminary, the INSERT image could be further improved through an updated calibration of the SPECT data. The calibration process must be carried out regularly. Due to the equipment required to calibrate the system, the process is not possible in the MRI environment. We set out to remove the system from the clinical MRI in order to update the calibration data and reconstruct improved images.

V. CONCLUSIONS

Multimodal imaging, especially when targeting large fields of view, requires several technical compromises. While PET/MRI is nowadays well consolidated [10], SPECT/MRI is still a niche and our work aims at fostering its development toward clinical use. High resolution SPECT/MRI scanners based on CdTe were realized for preclinical imaging [11] with excellent spatial and energy resolution, but limited FoV. We have successfully demonstrated the first clinical simultaneous SPECT/MRI imaging for brain oncology. The use of a commercial head coil has limited the choice of MRI sequences to only GRE. In perspective, the adoption of a shielded coil would widen the choice, as already shown for the preclinical scanner sharing the same design of the gamma cameras [5]. Very importantly, MRI imaging was here achieved with acceptable homogeneity despite the presence of the massive tungsten collimator. The intrinsic (1 mm) and extrinsic (10 mm) SPECT spatial resolution comply with the target specifications, while the energy resolution is worse than expected. This is partially due to the aging of the detectors

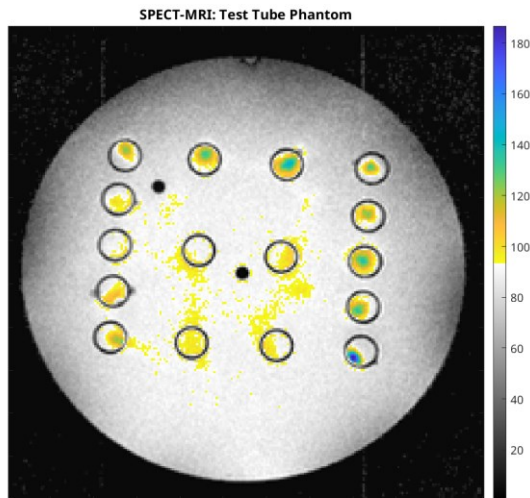


Fig. 4. Fig. 5. Combined SPECT-MRI data simultaneously acquired for 5 minutes with a GRE sequence: the color map (arbitrary units) shows MRI in the bottom half (gray scale) and SPECT on top (colors). The phantom covers the 20 cm diameter FoV, with 1 cm diameter test tube walls shown by the dark rings.

(manually assembled more than 5 years ago) and the repeated thermal cycles (from room temperature to -10°C). In fact, the most sensitive materials are the scintillators (hygroscopic), the wrapping foil (Teflon) and the optical glue coupling the scintillator with SiPM, whose properties directly impact on the energy resolution. We envision that enhanced performances can be achieved after updating and refreshing these materials.

ACKNOWLEDGMENTS

We gratefully acknowledge the support of Bart Maertens and Florian Odoj from Rapid Biomedical GmbH who provided the head coil for use with the INSERT system.

REFERENCES

- [1] B. F. Hutton, M. Occhipinti, A. Kuehne, D. Mathe, N. Kovacs, H. Waiczies, K. Erlandsson, D. Salvado, M. Carminati, G. L. Montagnani et al., "Development of clinical simultaneous spect/mri," *The British journal of radiology*, vol. 91, no. 1081, p. 20160690, 2018.
- [2] M. Occhipinti, M. Carminati, P. Busca, A. Butt, G. Montagnani, P. Trigilio, C. Piemonte, A. Ferri, A. Gola, T. Bukki et al., "Characterization of the detection module of the insert spect/mri clinical system," *IEEE Transactions on Radiation and Plasma Medical Sciences*, vol. 2, no. 6, pp. 554–563, 2018.
- [3] D. Salvado, K. Erlandsson, A. Bousse, M. Occhipinti, P. Busca, C. Fiorini, and B. F. Hutton, "Collimator design for a brain spect/mri insert," *IEEE Transactions on Nuclear Science*, vol. 62, no. 4, pp. 1716–1724, 2015.
- [4] M. Carminati, F. Baratelli, M. Occhipinti, K. Erlandsson, K. Nagy, Z. Nyitrai, M. Czeller, A. Kuehne, T. Niendorf, S. Valtorta et al., "Validation and performance assessment of a preclinical SiPM-based SPECT/MRI insert," *IEEE Transactions on Radiation and Plasma Medical Sciences*, vol. 3, no. 4, pp. 483–490, 2019.
- [5] M. Carminati, G. L. Montagnani, M. Occhipinti, A. Kuehne, T. Niendorf, K. Nagy, A. Nagy, M. Czeller, and C. Fiorini, "Spect/mri insert compatibility: Assessment, solutions, and design guidelines," *IEEE Transactions on Radiation and Plasma Medical Sciences*, vol. 2, no. 4, pp. 369–379, 2018.
- [6] I. D'Adda, A. J. Morahan, M. Carminati, K. Erlandsson, M. Ljungberg, B. F. Hutton, and C. Fiorini, "A statistical doi estimation algorithm for a sipm-based clinical spect insert," *IEEE Transactions on Radiation and Plasma Medical Sciences*, 2022.
- [7] B. Pedretti, S. Di Giacomo, L. Buonanno, I. D'Adda, C. Alaimo, M. Carminati, and C. Fiorini, "Experimental assessment of pca and dt classification for streamlined position reconstruction in anger cameras," *IEEE Transactions on Radiation and Plasma Medical Sciences*, 2022.
- [8] S. K. Øen, L. B. Aasheim, L. Eikenes, and A. M. Karlberg, "Image quality and detectability in siemens biograph pet/mri and pet/ct systems—a phantom study," *EJNMMI physics*, vol. 6, no. 1, pp. 1–16, 2019.
- [9] A. Morahan, K. Erlandsson, J. Dickson, I. D'Adda, M. Carminati, C. Fiorini, and B. F. Hutton, "Implications of the partial ring design for a clinical spect insert," in *2021 IEEE Nuclear Science Symposium and Medical Imaging Conference (NSS/MIC)*. IEEE, 2021, pp. 1–3.
- [10] V. Nadig, K. Herrmann, F. M. Mottaghy, and V. Schulz, "Hybrid totalbody pet scanners—current status and future perspectives," *European journal of nuclear medicine and molecular imaging*, pp. 1–15, 2021.
- [11] X. Lai, L. Cai, J.-W. Tan, E. M. Zannoni, B. Odintsov, and L.-J. Meng, "Design, performance evaluation, and modeling of an ultrahigh resolution detector dedicated for simultaneous spect/mri," *IEEE Transactions on Radiation and Plasma Medical Sciences*, vol. 6, no. 1, pp. 42–50, 2021.